25th ABCM International Congress of Mechanical Engineering
October 20-25, 2019, Uberlândia, MG, Brazil

COB-2019-1335
EVALUATION OF CARBON AND STAINLESS STEEL MICROWELDING: A CONTRIBUTION TO THIN SHEETS WELDING

Cledenir Costa de Oliveira
Claudio Abilio da Silveira
Rafael Gomes Nunes Silva
Max Baranenko Rodrigues
Calil Amaral
Milton Pereira
Universidade Federal de Santa Catarina, Mechanical Engineering Department, Precision Engineering Laboratory - Laser
cledenir.olveira@gmail.com
claudio_ards@hotmail.com
rafaelnunes.mat@hotmail.com
max.baranenko.ifsc@gmail.com
amaral.calil@gmail.com
milton.pereira@ufsc.br

Abstract. *In the present work the geometric profile of 316L stainless steel and AISI 1020 carbon steel weld beads were investigated. Twelve autogenous weld beads were manufactured in each material sample with an IPG Photonics continuous ytterbium fiber laser varying the welding speed and substrate material while maintaining fixed the other parameters. The main goals of this study were to evaluate and compare the behavior of each material under similar processing conditions, verify the existence of correlation between geometric and physical-chemical attributes of the weld beads and define optimum processing conditions. During the study, the width and penetration of the weld beads were measured and correlated with relevant physical-chemical characteristics. The surface profiles of the weld beads were analyzed in a Scanning Electron Microscope to observe possible weld discontinuities and their relationship with the assigned parameters.*

Keywords: *microwelding; AISI 1020 carbon steel; 316L stainless steel*

1. INTRODUCTION

Manufacturing, assembly, repair and maintenance of equipment are activities that are major components of project overall costs, schedules, robustness and feasibility. With the advent of new technologies, it was possible to develop manufacturing methods that are more efficient and enable the production of parts with better mechanical and metallurgical properties while reducing overall production costs by delivering batches with absence of defects. In this scenario, the use of a lasers as tool for processing materials is one of the most advanced methods occupying a prominent position in the industrial environment, according to Steen (2005).

One of the current widespread applications of conventional arc processes is joining dissimilar materials. This technique is applied in a variety of industries sectors, such as in nuclear power plants to connect stainless steel pipes with components made from low-carbon steels (Lima et Al., 2010). In order to explore the applicability of laser sources to weld dissimilar materials, it is of fundamental importance to understand the behavior and results of the interaction between the laser beam and each material individually. This study will then be focused on evaluating the weldability of stainless steel AISI 316L and low carbon steel AISI 1020 individually during the production of autogenous microwelds.

The complex physics involving laser matter interactions impose fundamental obstacles on the way to spread the use of laser welding techniques. Despite the complexities many authors have studied the combinations of a variety of factors, highlighting three of the most influential parameters that are responsible for defining the overall performance of laser microwelding processes: the power density, laser spot diameter and welding speed (Gapontsev, 2003).

Laser microwelding has become an important process in several industry sectors due to its many advantages over conventional processes such as arc welding. One of these advantages is the possibility to achieve elevated power densities on the melt pool, what leads to the production of weld beads with higher penetration depths. This advantage is particularly important when the process is used to join thin metal sheets, where the low power density of conventional arc welding

processes associated with the relatively small stiffness of thin sheets often result in distortions and warpage defects (D. Deng, et al, 2008) (D. Deng, et al, 2008).

Although some levels of geometrical distortions may not be noticed for thicker plates, they do have negative impact on assembly precision, aesthetic quality, mechanical and metallurgical properties of welds on thin sheets (S. Kou, 2003) (D. Deng, et al, 2008). In addition, correcting these defects is significantly expensive and, in some cases, becomes unfeasible or impossible to perform (K. Masubuchi, 1996). One possible solution to overcome these issues are the use of deep welding conditions, also known as penetration welding, a process condition that presents fewer thermal losses by conduction.

Penetration welding is a condition that, unlike conduction welding, is based on the formation of a metal vapor capillary, known as keyhole effect, in the melt pool. Poprawe (2011) indicated that the keyhole occurs when the incident power density (*I*) in the laser spot exceeds certain threshold values. For steels processed with gas- or solid-state-laser, for example, this threshold occurs when the power density is in the range of 1.0×10^6 W/cm² and 2.0×10^6 W/cm². In these processing conditions, the resulting weld beads present cross sections of high aspect ratios (penetration-to-width ratio) when compared to those produced by conduction welding.

The power density in laser welding processes is defined as the ratio between the power and the area of the beam on the surface of the workpiece. Similarly, the laser power divided by the welding speed result in the energy per unit length inserted in the weld bead, or linear input energy density (J/mm). These two values can be calculated in order to compare different configurations of equipment for welding. However, the welding behavior is susceptible to several factors that cannot always be expressed in terms of power density or linear energy density.

Changes in the dimensions of the melting pool are caused by the variation of welding speed for same power density conditions. At high speeds a keyhole elongation will occur due to the decrease of the liquid phase in its surroundings that results from different cooling conditions. Another effect is the formation of rounded protuberances on the outer surface of the weld bead, known as the humping effect, that are resultant from high flow rates of the molten material to the end of the melt pool as illustrated by Patschger *et al.* (2014).

The dynamics of the melt pool is also influenced by the laser spot size on the surface of the workpiece. As an example, larger spot diameters result in more melted material for same energy densities, however the resulting weld bead geometry will be different due to other factors such as the influences of surface tension on the behavior of the pool (Kim *et al.*, 2016).

As a first approach to understand the physics behind the laser microwelding of AISI 1020 carbon steel and 316L stainless steel thin sheets, the present study documents qualitative and quantitative parameters resulting from the manufacture of a total of twenty-four autogenous weld beads. The bead penetration depth and width of the weld beads, as well as the aspect ratio and threshold processing conditions prior to the formation of humps were the main characteristics evaluated and will be further discussed in the following sessions.

2. MATERIALS AND METHODS

An YG-400-AC-Y14 IPG Photonics yttrium fiber laser with a maximum power of 400 W and wavelength of 1070 nm was used. A collimator with a focal length of 50 mm at the end of the fiber, provided a collimated bundle with diameter of 6,9 mm and M² of 1,2. The laser beam movement was performed by an HPO-14 AEROTECH galvanometer scanner equipped with an F-theta lens with a focal length of 170 mm. The theoretical diameter of the laser focal point for this configuration is 58 μm.

Table 1- Chemical and physical properties of the materials used

Property	Material			
	AISI 1020 Carbon Steel		316L Stainless Steel	
Chemical Composition (wt %)	Mn	0,3 - 0,6	Mn	2 (max)
	C	0,18 - 0,23	C	0.03 (max)
	S	0,05 (max)	Cr	16 - 18
	P	0,04 (max)	Ni	10 - 14
	Fe	Remaining	Mo	2 - 3
			Si	1 (max)
			Si	0.03 (max)
			P	0.045 (max)
			Fe	Remaining
Thermal Conductivity (W/mK)	51.9		16.3	

AISI 1020 carbon steel plates and 316L stainless steel with a thickness of 1.2 mm were used in the work. The chemical and physical properties of these materials can be consulted in Table 1. For each sample material, twelve autogenous weld beads were manufactured. The power was fixed in 400 W and the welding speed varied from 100 mm/s to 1200 mm/s, with increments of 100 mm/s between the tests. The focal plane of the laser beam was set to coincide with the top surface of the samples. In order to reduce the number of variables between the tests, no protection gas flow was used. The

equipment exhaust system was employed to avoid the accumulation of process fumes in the optical path of the laser beam. A delay of 2 s between the completion of each bead was included to avoid heating the sample.

The samples were cut to reveal the cross section of the weld beads. The metallographic preparation was carried out with sanding, polishing with diamond paste and chemical etching by immersion. The carbon steel sample was attacked with Nital reagent (2%) and the stainless-steel sample with Marble reagent. The images were collected on an Olympus BX60M microscope and evaluated with a scanning electron microscope, model HITACHI TM-3030. The measurements were performed on the ImageJ ® software. The width and penetration of the region comprising the weld bead were measured. In cases where total penetration was observed, the thickness of the substrate was considered.

3. RESULTS AND DISCUSSIONS

After the measurement of width and penetration of each weld bead, Table *2* was consolidated to numerically summarize the conditions of each experimental run and relate it with the geometrical aspects of the respective resulting cross section.

Table 2 – Experimental conditions and geometrical characteristics of the resulting cross sections.

	316L Stainless Steel				AISI 1020 Carbon steel				
Welding speed (mm/s)	**Weld sample**	**Penetration (mm)**	**Width (mm)**	**Aspect ratio**	**Weld sample**	**Penetration depth (mm)**	**Width (mm)**	**Aspect ratio**	**Schematics of penetration and width measurement**
100	A.1	1.200	0.276	4.348	B.1	1.200	0.421	2.853	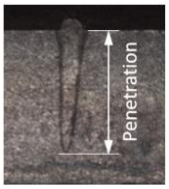
200	A.2	1.200	0.195	6.154	B.2	1.200	0.365	3.289	
300	A.3	0.940	0.192	4.894	B.3	1.005	0.287	3.502	
400	A.4	0.838	0.156	5.369	B.4	0.923	0.256	3.605	
500	A.5	0.640	0.151	4.236	B.5	0.869	0.208	4.178	
600	A.6	0.601	0.140	4.294	B.6	0.823	0.187	4.401	
700	A.7	0.598	0.128	4.669	B.7	0.789	0.158	4.994	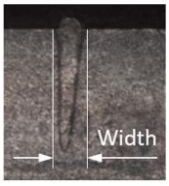
800	A.8	0.536	0.120	4.470	B.8	0.721	0.136	5.301	
900	A.9	0.514	0.118	4.353	B.9	0.685	0.128	5.352	
1000	A.10	0.458	0.110	4.167	B.10	0.663	0.115	5.783	
1100	A.11	0.421	0.098	4.298	B.11	0.587	0.098	5.990	
1200	A.12	0.384	0.082	4.683	B.12	0.523	0.087	6.011	

The results comprise a range of penetrations that vary from 0.384mm for 316L stainless steel at high welding speeds to full penetration (1.200 mm) for speeds lower than 200 mm/s. The lowest penetration achieved for AISI 1020 carbon still was 0.523mm at 1200 mm/s with full penetration also happening for 200 mm/s and lower welding speeds. Similarly, high welding speeds resulted in the smallest bead width, with AISI 1020 and 316L stainless steel presenting 0.087 mm and 0.082 mm of width respectively. Figure *1* and Figure 2 summarizes these characteristics showing that the bead dimensions tend to decrease with increasing welding speeds as well as evidences greater dimensions for the AISI 1020 carbon steel.

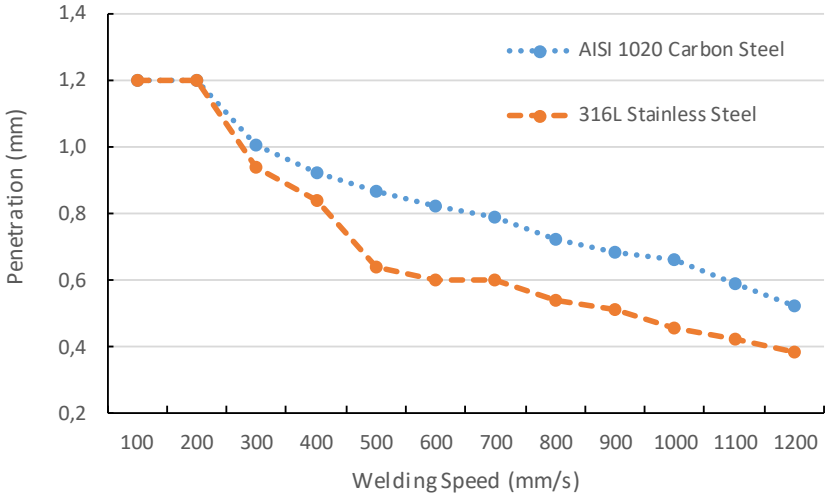

Figure 1 – Penetration depth achieved under different welding speed conditions for the microwelding of AISI 1020 carbon steel and 316L stainless steel.

The experiments leave no doubts about being easier to achieve higher penetrations with the same values of input linear energy density for welds made in AISI 1020 carbon steel than in 316L stainless steel. As for welding speeds of 200 mm/s and below, resulting in the highest input liner energy density, the penetration was limited by the thickness of the metal samples and no further conclusions can be drawn except that full penetration was obtained for both materials.

The trends observed in Figure 2 can be explained by the amount of heat input absorbed per unit length of the weld bead. At low speeds the laser beam delivers more energy per unit length, resulting in high linear energy densities for both materials and higher bead penetrations. Similarly, at high speeds the laser spot spends less time at each location along the length of the bead, what results in decrease of linear energy density and consequently decrease in bead penetrations.

In an analogous way, the widths of the weld beads obtained by the procedures can be analyzed. The same relationship between bead width and linear power density can also be observed in this study and are illustrated in Figure 2 but with a lower variation between the values obtained. The combination of these geometrical parameters highlights the high ratio between penetration and width obtained through the laser welding process. Although the trend of decreasing dimensions for increasing speeds is the same for the different materials, the results are different between them, what can be explained paying closer attention to some physical properties.

Laser welding processes are influenced by several physical-chemical properties of the materials. The surface finish of the workpieces affects the index of reflectivity and consequently impacts the absorption of laser energy by the workpiece. In addition, the thermal conductivity is one of the characteristics that defines how heat is transferred through the material and can have an important influence on weldability indicators.

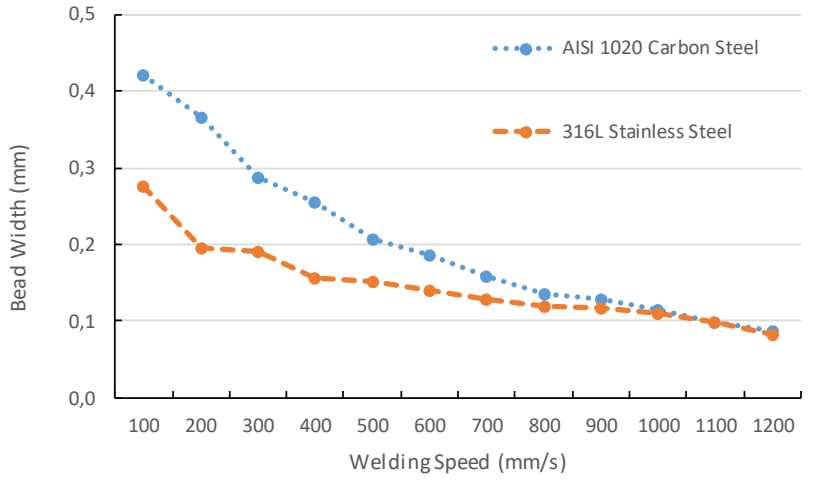

Figure 2 – Bead width achieved under different welding speed conditions for the microwelding of AISI 1020 carbon steel and 316L stainless steel.

The materials used for this study presented different values of thermal conductivities, with AISI 1020 carbon steel being almost three times better than 316L in transferring heat by conduction. This factor alone could help to explain the

greater penetrations achieved in AISI 1020 for same linear input energy density levels. The greater reflectivity of the 316L could also indicate that a greater portion of the energy was reflected, resulting in smaller observable areas that went through phase change. Although no quantitative method was used to characterize the reflectivity of the samples, the higher brightness of the optical macrographs illustrated in Figure 3 (b) and (d) offer good evidences that the 316L stainless steel reflect more light then AISI 1020 samples (a) and (c).

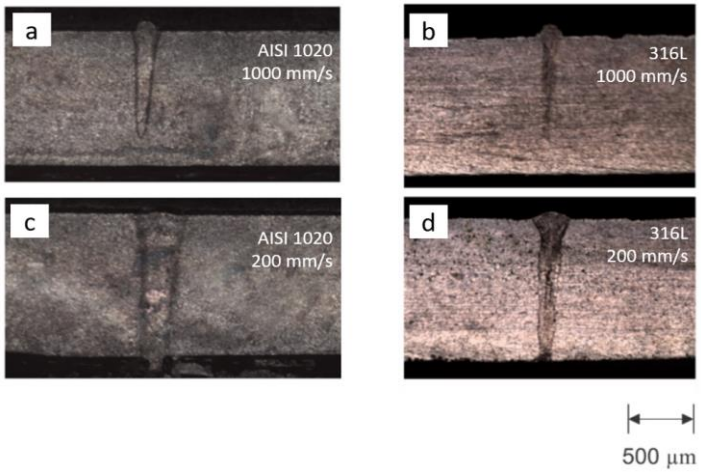

Figure 3 - Macrographs of samples processed with 400 W of power. (a) AISI 1020 carbon steel with 1000 mm/s weld speed; (b) 316L stainless steel and 1000 mm/s weld speed; (c) AISI 1020 carbon steel with 200 mm/s weld speed; (d) 316L stainless steel and 200 mm/s.

According to the literature, one of the greatest advantages of the laser welding process when compared with arc welding is the potential to create weld beads with high aspect ratios between penetration depth and transversal width. For deep welding, this characteristic can bring evidences of the processing conditions during the joining procedures. For the present study the weld beads produced, resulted in the aspect ratios illustrated in Figure 4.

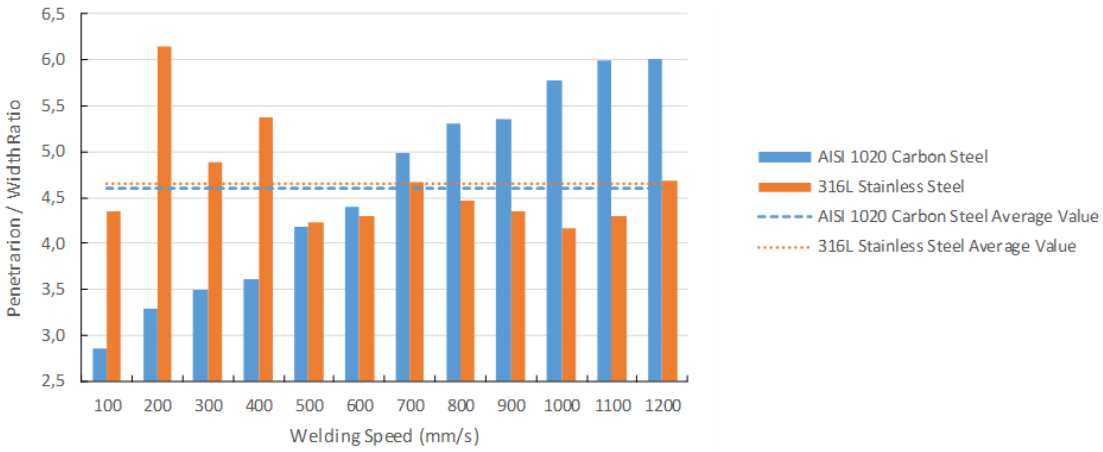

Figure 4 – Ratio between penetration depth and width for different materials and welding speeds.

Two aspects can be observed by analyzing the penetration-to-width ratio of the weld beads produced. The first is the average value calculated for the two materials, a parameter that can be considered for future comparisons between welding processes. For both AISI 1020 carbon steel and 316L stainless steel, the resulting average value was close to 4.6 (4.605 and 4.661 for AISI 1020 carbon steel and 316L stainless steel respectively). The second aspect observed is the clear tendency of the penetration-to-width ratio to increase in AISI 1020 carbon steel for increasing values of welding speed, whereas 316L exhibit a negative trend for increasing welding speeds.

Finally, from the microscopy analysis, it was possible to notice the formation of humps on the surface of the weld beads for certain weld speed ranges. The humping effect was consistently observed in 316L stainless steel samples produced with weld speeds ranging from 600 to 1200mm/s. The same effect was observed in AISI 1020 carbon steel samples produced with weld speeds varying from 700 to 1200 mm/s. Figure 5 schematically shows the correlation between the weld speeds and the formation of humps for the studied materials.

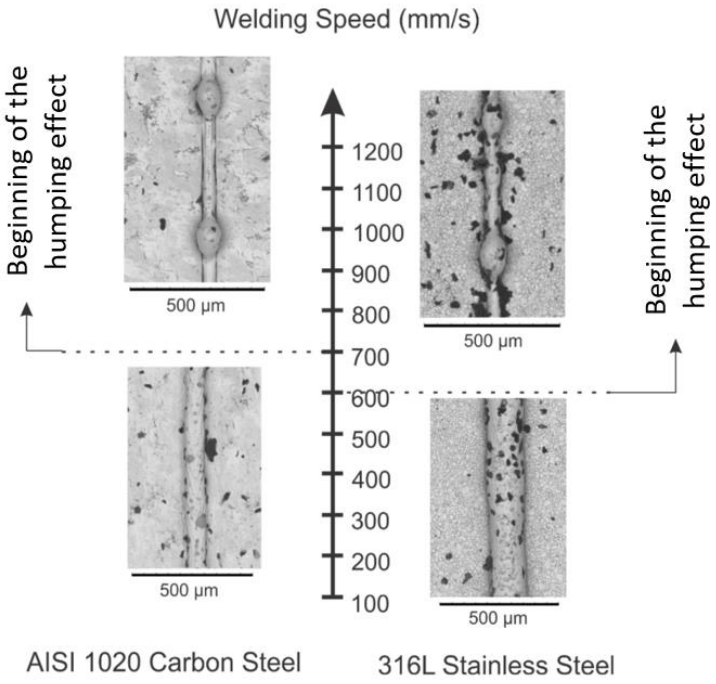

Figure 5 – Welding speed threshold values for the formation of humps in weld beads of different materials.

4. CONCLUSIONS

The system used with its optical configuration, together with the parameters of power and welding speed, allowed the welding and analysis of the geometric profiles of the weld beads.

Through these, it is possible to correlate the results obtained with the physical-chemical characteristics of the materials used. This correlation is of major importance in the choice of optimized parameters for a given application, either to obtain total or partial penetration. Among the analyzed parameters, penetrations were obtained from 0.384 mm to total penetration for 316L stainless steel, and from 0.421 mm to penetration for AISI 1020 carbon steel.

It was possible to observe undesirable formation of humps on the surface of the weld beads. The humping effect, as reported in the literature, was observed for welding speeds ranging from 700 to 1200 mm/s for AISI 1020 carbon steel and from 600 to 1200 mm/s for 316L stainless steel samples.

Moreover, it was possible to reproduce the high penetration-to-width ratio through the laser welding process, which is considered an inherent advantage of the process when compared to traditional welding processes. This average value of penetration and width ratio obtained for both materials were 4.6 and could be a qualitative artifice for future comparison between different welding processes.

5. ACKNOWLEDGEMENTS

The authors would like to thank the National Council for Scientific and Technological Development (CNPq – Brazil) for the support.

6. REFERENCES

Deng, D. and Murakawa, H.: Prediction of Welding Distortion and Residual Stress in a Thin Plate Butt-welded Joint, Computational Materials Science, (2008), Vol. 43, 353-365.

Gapontsev, V.: Industrial applications of high-power fiber lasers, Proc. Advances in Fiber Lasers, Photonic West (2003)

Kim, J.; Kim, S.; Kim, K.; Jung, W.; Youn, D.; Lee, J.; Ki, H.; Effect of beam size in laser welding of ultra-thin stainless-steel foils. Journal of Materials Processing Technology, 233, 125-134, 2016.

S. Kou, Welding Metallurgy, 2nd edition (New York: John Wiley, 2003), pp. 263–339.

Lima, L. I. L.; Silva G. M.; Chilque A. R. A.; Schvartzman, M. M. A. M.; Bracarense, A. Q.; Qquinan, M. A. D.; Caracterização Microestrutural De Soldas Dissimilares Dos Aços Astm A-508 E AISI 316L, Soldagem Insp. São Paulo, v. 15, n. 2, p.112-120, Abr-Jun 2010.

Masubuchi, K.: Prediction and Control of Residual Stresses and Distortion in Welded Structures, Transactions of JWRI, (1996), Vol. 25, No. 2, 53-67.

Patschger, A.; Bliedtner, J.; Bergmann, J. P.; Process-limiting Factors and Characteristics of Laser-based Micro Welding. Physics Procedia, 56, 740-749, 2014.

Poprawe, R.; Tailored Light 2: Laser Application Technology, Springer-Verlag Berlin Heidelberg.; 2011.

Radaj, D.: Heat Effects of Welding, Springer-Verlag, (1992), 1, 9-11, 14, 149.

Steen, W. M. Laser Material Processing. Ed. Springer-Verlag. 3a ed., ISBN 1852336986. 2005.

7. RESPONSIBILITY NOTICE

The authors are the only responsible for the printed material included in this paper.